Hydrogen Atom Transfer Reactions of C_2^-, C_4^-, and C_6^-: Bond Dissociation Energies of Linear $H-C_{2n}^-$ and $H-C_{2n}$ ($n = 1, 2, 3$)

Yang Shi[†] and Kent M. Ervin*

Department of Chemistry and Chemical Physics Program, University of Nevada, Reno, 1664 North Virginia Street, Reno, Nevada 89557-0216

Received: September 6, 2007; In Final Form: October 16, 2007

The reactions of C_2^-, C_4^-, and C_6^- with D_2O and ND_3 and of C_4^- with CH_3OH, CH_4, and C_2H_6 have been investigated using guided ion beam tandem mass spectrometry. Hydrogen (or deuterium) atom transfer is the major product channel for each of the reactions. The reaction threshold energies for collisional activation are reported. Several of the reactions exhibit threshold energies in excess of the reaction endothermicity. Potential energy calculations using density functional theory show energy barriers for some of the reactions. Dynamic restrictions related to multiple wells along the reaction path may also contribute to elevated threshold energies. The results indicate that the reactions with D_2O have the smallest excess threshold energies, which may therefore be used to derive lower limits on the C−H bond dissociation energies of the $C_{2n}H^-$ and $C_{2n}H$ ($n = 1-3$) linear species. The experimental lower limits for the bond dissociation energies of the neutral radicals to linear products are $D_0(C_2-H) \geq 460 \pm 15$ kJ/mol, $D_0(C_4-H) \geq 427 \pm 12$ kJ/mol, and $D_0(C_6-H) \geq 405 \pm 11$ kJ/mol.

1. Introduction

Polyynyl radicals, $C_{2n}H$, have received extensive study because of their importance in combustion processes[1−3] and astrophysical environments.[4−7] Although these radicals have been characterized spectroscopically[8−15] and theoretically,[16−22] the $C_{2n}-H$ bond dissociation energies are not experimentally well-established. Accurate theoretical calculation of the energies is also problematic because of the complex electronic structures of $C_{2n}H$ radicals, which have low-lying $^2\Sigma$ and $^2\Pi$ electronic states mixing acetylenic and cumulenic electronic structures.[1,18,19,21] Pure rotational spectra of the negative ions $C_{2n}H^-$ ($n = 2, 3, 4$) have recently been detected in the laboratory and interstellar space,[23−26] among the first molecular anions identified in astronomical sources. While the electron affinities of the polyynyl radicals are accurately known,[8−10,27,28] the C−H bond dissociation energies of the anions are poorly established.

In this work, we use guided ion beam tandem mass spectrometry[29] to measure the reaction threshold energies for hydrogen atom transfer reactions of C_{2n}^- ($n = 1-3$), reaction 1.

$$C_{2n}^- + HX \rightarrow HC_{2n}^- + X \tag{1}$$

The HX (or DX) neutral reagents employed are D_2O, ND_3 for $n = 1$, 2, and 3 and also CH_4, C_2H_6, and CH_3OH for $n = 2$. The measured reaction threshold energy, E_0, for collisional activation of reaction 1 is an upper limit for the true reaction endothermicity, which can be related to the bond dissociation energies of HX and HC_{2n}^- according to eq 2.

$$E_0 \geq \Delta H_0 = D_0(H-X) - D_0(H-C_{2n}^-) \tag{2}$$

When $D_0(H-X)$ is known, the measured threshold energy provides a lower limit for the bond dissociation energy of HC_{2n}^-, eq 3.

$$D_0(H-C_{2n}^-) \geq D_0(H-X) - E_0 \tag{3}$$

The C−H dissociation energy of the neutral radical can then be obtained from the anionic value via eq 4,[30]

$$D_0(H-C_{2n}) = D_0(H-C_{2n}^-) + EA_0(C_{2n}) - EA_0(HC_{2n}) \tag{4}$$

using electron affinities that have been measured by photoelectron spectroscopy.[8−10,27,28] The experimental lower limit for $D_0(H-C_{2n}^-)$ therefore also gives a lower limit for $D_0(H-C_{2n})$. The H−X bond dissociation energies and electron affinities for C_{2n} and HC_{2n} are summarized in Table 1 along with other relevant literature thermochemistry.[8−10,27,28,31−38]

Only limited information about hydrogen atom transfer reactions of carbon cluster anions is available. Bohme[39,40] found that the reactions of C_2^- with H_2O, CH_4, and H_2 have rate constants less than their measurement limit of 10^{-12} to 10^{-13} $cm^3\ s^{-1}$. Bierbaum and co-workers[41] found that the reactions of C_x^- ($x = 2$, 4−10) with molecular H_2 are immeasurably slow at room temperature, $k < 10^{-13}$ $cm^3\ s^{-1}$. To our knowledge, the only reported hydrogen atom transfer reactions of C_{2n}^- ($n = 1-3$) anions are with H_2S for C_4^- and C_6^-, which react near the collision rate to form $C_{2n}H^-$ and HS^- as the major products,[42,43] and with benzenethiol for C_4^- giving HC_4^- as a minor product channel.[43]

Endothermic ion−molecule reactions activated by translational energy often exhibit a threshold energy equal to the thermochemical endothermicity, providing an important means for ion thermochemistry determinations.[30,44,45] Strictly, however, the reaction threshold energy is an upper limit for $\Delta_r H$. Endothermic and thermoneutral S_N2 reactions of anionic halide

* To whom correspondence should be addressed. E-mail: ervin@unr.edu.
[†] Current address: SDSD, Kodak Co., San Diego, CA 92127.

10.1021/jp077181c CCC: $40.75
Published on Web 01/23/2008

TABLE 1: Literature Thermochemical Values

species	D_0/kJ mol^{-1}	ref
HO−H	492.01 ± 0.29	37
DO−D	501.2 ± 0.4	*a*
N_2N−H	444.1 ± 1.1	37
D_2N−D	454.8 ± 1.2	*a*
CH_3−H	432.72 ± 0.14	37
CH_3O−H	434.6 ± 2.2	37
C_2H_5−H	416.7 ± 1.0	38

	EA_0 (exp)/eV	ref	EA_0 (theory)[a,b]
C_2 ($^1\Sigma$)	3.269 ± 0.006	8	3.224
C_2H ($^2\Sigma$)	2.969 ± 0.006	8	2.993
	2.956 ± 0.020	9	
C_4 ($^3\Sigma$)	3.882 ± 0.010	27	3.873
C_4H ($^2\Sigma$)	3.561 ± 0.010	10	3.653
	3.558 ± 0.015	9	
C_6 ($^3\Sigma$)	4.180 ± 0.001	28	4.223
C_6H ($^2\Pi$)	3.796 ± 0.005	10	3.971[c]
	3.809 ± 0.015	9	

	D_fH_0/kJ mol^{-1}	D_fH_{298}/kJ mol^{-1}	ref
C_2 ($^1\Sigma$)	817 ± 8	817 ± 10[a]	36
C_4 ($^3\Sigma$)	1052 ± 16	1062 ± 16[a]	36
C_6 ($^3\Sigma$)	1312 ± 18	1327 ± 18[a]	34
HCCH	228.0 ± 0.8	227.2 ± 0.8	32
HC_4H	449 ± 20[a,d]	450 ± 20[d]	33
HC_6H	666 ± 40[a,d]	670 ± 40[d]	33

[a] Isotopic vibrational zero-point energy corrections and thermal enthalpy corrections use unscaled frequencies from B3LYP/aug-cc-pVTZ calculations (see Supporting Information) and reference state values from Gurvich et al.[32] [b] This work, CCSD(T)/aug-cc-pVQZ//CCSD(T)/aug-cc-pVTZ except as noted. The ground electronic states of C_{2n}^- and HC_{2n}^- are $^2\Sigma$ and $^1\Sigma$, respectively. [c] CCSD(T)/aug-cc-pVQZ//B3LYP/aug-cc-pVTZ. [d] Group additivity estimates.

atoms, for example, with a double-well potential and central barrier along the reaction path exhibit dynamic restrictions for translational activation that raise the observed threshold energies above the endothermicity or barrier height.[29,46,47] In this work, we employ density functional theory calculations of the potential energy surfaces for hydrogen atom transfer reactions to elucidate the reaction dynamics and we report coupled-cluster calculations of energies for comparison with experimental values.

2. Experimental Methods

Experiments are performed with our guided ion beam tandem mass spectrometer, which has been described previously.[29] The pure carbon cluster anions C_{2n}^- ($n = 1, 2, 3$) are generated by a microwave discharge with acetylene as precursor gas and helium as buffer gas. For C_2^-, an alternative method is also applied, in which O_2 is the precursor gas to generate O^- in the microwave discharge and C_2H_2 is added downstream. Acetylene and O^- react to form C_2^- among other species.[8] The ions are thermalized to room temperature by $\sim 2 \times 10^5$ collision in the flow tube ($\sim$350 mTorr helium).

The structures of C_4^- and C_6^- generated in our ion source are certainly linear. Photoelectron spectroscopy of C_4^- and C_6^- using various sources (laser vaporization of graphite[27,48] and pulsed electric discharge of C_2H_2 and CO_2)[49] identify only the linear species. Ion chromatography with a laser vaporization source[50] also found only linear species for C_x^- ($x = 5-9$). Theoretical calculations[51,52] indicate that C_x^- clusters are linear up to $x = 9$. Some ring and bent structures do exist in high level ab initio calculations on the anions,[51,53−55] but the most stable isomer is about 130 kJ/mol higher than the linear structure. Under our thermal source conditions at 300 K, such high energy isomers will not exist. Hence, we may assume that all generated C_4^- and C_6^- ions are linear. Calculations[56,57] indicate that the first electronically excited states of C_4^- and C_6^- are 1.24 and 2.15 eV higher than their ground states, respectively, and are therefore unlikely to be present. The $A^2\Pi$ excited-state of state of C_2^- lies at 0.49 eV, however, and has been shown by photoelectron spectroscopy to be populated in a similar flow tube reactor source.[8]

The desired carbon cluster anions are mass selected by a magnetic sector mass spectrometer and injected into a radio frequency octopole ion beam guide at a set translation energy, where the anions react with the target gas. Reactant and product anions are collected by the octopole and mass analyzed by a quadrupole mass spectrometer and channeltron ion detector. Reaction cross-sections are calculated from the relative abundances of reactant and product ions.[58] The laboratory ion energy is measured by retarding energy analysis and verified by a time-of-flight measurement[59] and then converted to the relative collision energy in the center-of-mass (c.m.) frame.[58] To obtain strictly single-collision conditions, the cross sections are measured at three reactant gas pressures in the gas cell and extrapolated to zero pressure.

The single-collision reaction cross section, $\sigma(E)$, is modeled with the CRUNCH program[60] using an empirical threshold law,[58,59]

$$\sigma(E) = \frac{\sigma_0}{E} \sum_i g_i (E + E_i - E_0)^N \qquad (5)$$

where E_i is the internal energy of reactant state i with fractional Boltzmann population g_i, σ_0, and N are adjustable parameters, and E_0 is the 0 K reaction threshold energy. Equation 5 is further convoluted over the thermal motion of the target gas (300 K) and the measured ion kinetic energy distribution (0.15−0.25 eV full-width at half-maximum typical) using the double integral method.[58,61] The parameters σ_0, N, and E_0 are obtained by a nonlinear least-squares fit of the model to the data.

The vibrational and rotational frequencies of the reactants used for the internal energy calculations are taken from calculations, as summarized in the Supporting Information. It is generally accepted that reactant vibrational energy is available to promote endothermic ion−molecule reactions near the reaction threshold energy and should be included in eq 5 to obtain accurate 0 K threshold energies.[62,63] However, the role of rotational energy is still an open question.[63] Because inclusion of rotational energy as fully available for promoting reaction raises the apparent 0 K threshold energy that results from fitting eq 5, for the purposes of this work, we include rotational energy to obtain E_0 as an *upper limit* for ΔH_0. If it is determined later that rotational energy should not be included, then the reported E_0 values should be systematically reduced (and the bond dissociation energy limits increased) by about 6.2 kJ/mol (2.5 RT).

3. Hydrogen Atom Transfer Threshold Energies

Figures 1−3 show the single-collision cross sections for reaction (1). Hydrogen atom transfer to form HC_{2n}^- is the main product channel for C_{2n}^- ($n = 1, 2, 3$) reacting with the various neutral reagents. For $C_4^- + CH_3OH$, a weak CH_3O^- product is also observed with a threshold energy of about 3 eV, well above the threshold for HC_4^-; this minor process is not considered further here. Reaction threshold energies, E_0, from the fits of eq 5 are presented in Table 2.

For the reactions of C_2^- with D_2O and ND_3 (Figure 1), a small reaction cross section for HC_2^- at low energies that

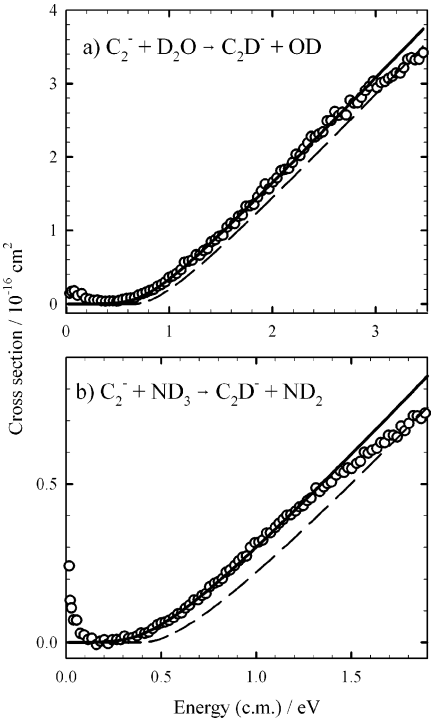

Figure 1. Deuterium atom transfer cross sections for reaction of C_2^- with (a) D_2O and (b) ND_3 (circles). Solid lines show the fits to the data described in text and dashed lines show the cross section model without energy convolutions.

decreases with increasing energy is observed in addition to the main endothermic channel that rises from the threshold. Pulsing the ion beam, which would remove collisionally slowed ions that might become trapped in the octopole,[64] was applied and the feature was still present, eliminating trapped ions as a possible source of the low-energy feature. The low-energy behavior may therefore be associated with an exothermic process. An alternative ion formation method, C_2^- made from the $C_2H_2 + O^-$ reaction, was applied to react with D_2O with both pulsed and continuous modes. Both features are still present, although the relative magnitude of the low-energy feature varies somewhat with ion source conditions. These observations are consistent with having a small portion of the C_2^- ion beam in an internally excited state, presumably the $C_2^-(A^2\Pi_u)$ electronic state mentioned above. Because the cross section of the low-energy feature goes to zero below the threshold of the endoergic process, its presence does not affect our threshold energy determinations for the ground state.

The reported uncertainties for E_0 for the D_2O and ND_3 reactions represent estimates of ±2 combined standard uncertainties.[65] The error bars include the uncertainties for the laboratory ion energy measurement, the statistical error from the least-squares fits, the uncertainty of molecular parameters in the model (±15% for calculated frequencies), the reproducibility of data taken on multiple occasions, and the reproducibility of the threshold fits over various energy ranges. For the other neutral reactants, only one or two experiments were performed and the uncertainty is estimated conservatively at ±0.2 eV.

The measured reaction threshold energies may be used to derive lower limits to the bond dissociation energies for HC_{2n}^- using eq 3. The results are presented in Table 2 for each reaction. The lower limits for $D_0(H-C_{2n}^-)$ are highest from the reactions with D_2O, which indicates that the other reactants definitely have apparent threshold energies in excess of the reaction (1)

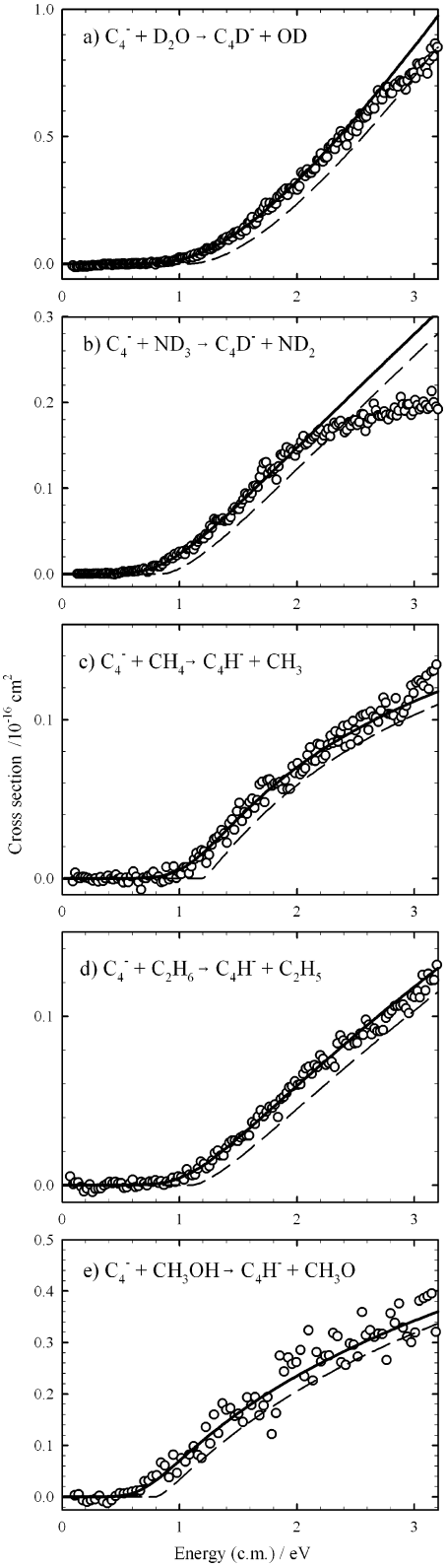

Figure 2. Hydrogen or deuterium atom transfer cross sections for reaction of C_4^- with (a) D_2O, (b) ND_3, (c) CH_4, (d) C_2H_6, and (e) CH_3OH (circles). Solid lines show the fits to the data described in text and dashed lines show the cross section model without energy convolutions.

endothermicity, by amounts ranging from at least 20 to 85 kJ/mol. This of course does not exclude the possibility that the $C_{2n}^- + D_2O$ reactions might also have threshold energies in excess of their endothermicities.

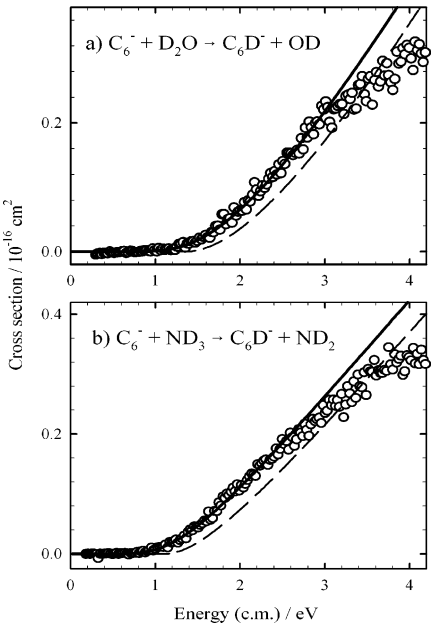

Figure 3. Deuterium atom transfer cross sections for reaction of C_6^- with (a) D_2O and (b) ND_3 (circles). Solid lines show the fits to the data described in text and dashed lines show the cross section model without energy convolutions.

TABLE 2: Threshold Energies (eV) for Hydrogen (deuterium) Atom Transfer Reactions $C_{2n}^- + HX \rightarrow C_{2n}H^- + X$ ($n = 1-3$)

reactants	E_0/eV	D_0(H[D]−C_2^-)[a]/kJ mol^{-1}
$C_2^- + D_2O$	0.67 ± 0.15	>431 ± 15 [>437 ± 14]
$C_2^- + ND_3$	0.40 ± 0.06	>410 ± 6 [>416 ± 6]
$C_4^- + D_2O$	1.02 ± 0.13	>396 ± 12 [>403 ± 12]
$C_4^- + ND_3$	0.84 ± 0.10	>367 ± 10 [>374 ± 10]
$C_4^- + CH_4$	1.2 ± 0.2	>317 ± 20
$C_4^- + CH_3OH$	0.8 ± 0.2	>357 ± 20
$C_4^- + C_2H_6$	1.1 ± 0.2	>311 ± 20
$C_6^- + D_2O$	1.29 ± 0.11	>370 ± 11 [>377 ± 11]
$C_6^- + ND_3$	1.03 ± 0.16	>348 ± 15 [>355 ± 15]

[a] Lower limits for anion bond dissociation energy, calculated using eq 3 and neutral reactant bond dissociation energies from Table 1. Isotopic vibrational zero-point energy corrections using unscaled harmonic frequencies calculated at the B3LYP/aug-cc-pVTZ level (see Supporting Information).

4. Potential Energy Surfaces

We have examined the potential energies along the hydrogen atom transfer reaction path using density functional theory at the B3LYP/aug-cc-pVDZ level[66−69] for the example systems $C_2^- + HX \rightarrow HC_2 + X^-$ (HX = H_2O, NH_3, and CH_4). This level of theory is sufficient for determining the general topology of the reaction paths although the energies are approximate. The resulting energy level diagrams are shown in Figure 4. Stationary points were confirmed with frequency calculations at the same level. The connections between stationary points have been verified with a combination of Intrinsic Reaction Coordinate[70] calculations and constrained potential energy surface scans, although we have not necessarily identified all local minima and conformations.

Each of the three systems passes through an initial minimum in the entrance channel corresponding to a C_2^-(HX) ion−molecule complex followed by a maximum corresponding to the [CC···H···X]$^-$ transition state for hydrogen atom transfer.

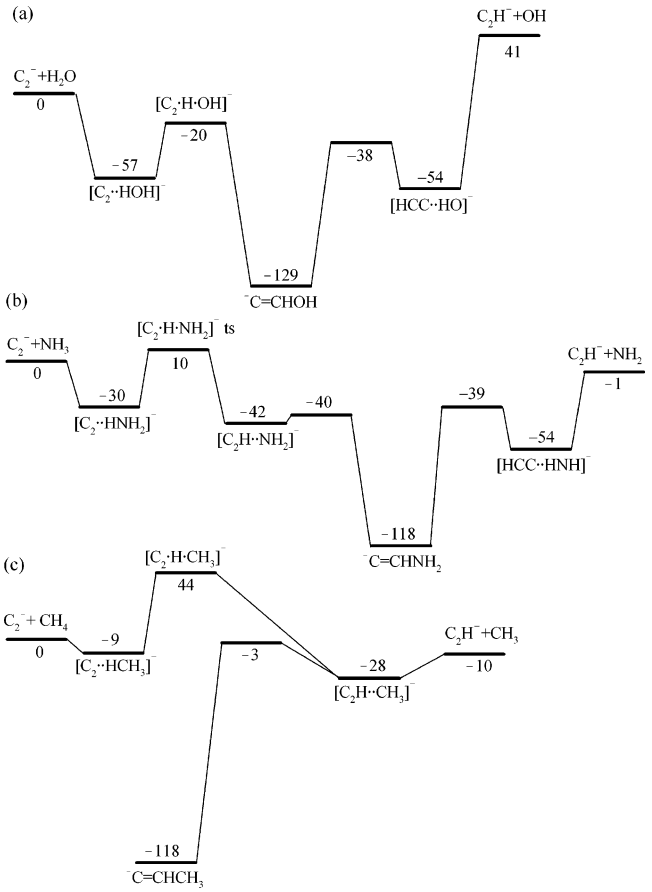

Figure 4. Energy level diagrams of the potential energy surfaces for the hydrogen atom transfer reactions between (a) $C_2^- + H_2O$, (b) $C_2^- + NH_3$, and (c) $C_2^- + CH_4$. Energies relative to reactants (kJ/mol) are given at the B3LYP/aug-cc-pVDZ level without zero-point energy corrections.

The height of the barrier relative to reactants is −20 kJ/mol for H_2O, 10 kJ/mol for NH_3, and 44 kJ/mol for CH_4 (not corrected for zero-point energies). That is, the energy of the central barrier is below reactants and products for H_2O, but is higher than reactants and products for NH_3 and CH_4. The high energy of the hydrogen atom transfer transition state for NH_3 and CH_4 partly explains the excess threshold energies for those reactions, although the observed magnitudes are higher than the calculated barrier heights. Similar behavior was observed[29] for the thermoneutral S_N2 reaction $Cl^- + CH_3Cl \rightarrow Cl\,CH_3 + Cl^-$, which has a double-well potential with a central barrier height of 10−13 kJ/mol but an observed threshold energy of 45 kJ/mol. Dynamic constraints for translation activation of the S_N2 reaction result in a elevated threshold energy.[29,47] For $C_2^- + H_2O$, reaction is possible once translational energy equal to thermochemical endothermicity is supplied because the transition state barrier lies below reactants. However, it is known that a potential energy barrier along the reaction path can result in dynamic restrictions even if it lies below the product energy,[71] so the apparent reaction threshold energy is strictly still an upper limit to the reaction endothermicity. Futhermore, for the same reasons the magnitude of the observed theshold energies for translational activation only give upper limits for the potential energy barrier heights.

The $C_2^- + HX$ potential energy surfaces exhibit qualitative differences (H_2O, NH_3, and CH_4) beyond the barrier for hydrogen atom transfer. For H_2O, there is a deep well in the exit channel corresponding to the covalently bound $^-$C═CHOH

TABLE 3: Bond Dissociation Energies (kJ mol^{-1})

value	$n = 1$	$n = 2$	$n = 3$	method
$D_0(H-C_{2n}^-)$	$>431 \pm 15$	$>396 \pm 12$	$>370 \pm 11$	exp[a]
	442.2	438.7	438.2	theory[b]
$D_0(H-C_{2n})$[c]	$>460 \pm 15$	$>427 \pm 12$	$>405 \pm 11$	exp[d]
	464.5	459.9	461.8[e]	theory[b]
	471	470	474	exp/theory[b,f]
$D_{298}(H-C_{2n})$[c]	488	385	360	thermo[g]

[a] From threshold energies for reactions with D_2O (Table 2). [b] Energies from CCSD(T)/aug-cc-pVQZ//CCSD(T)/aug-cc-pVTZ calculations, except as noted, with zero-point energy corrections from unscaled harmonic vibrational frequencies at the B3LYP/aug-cc-pVTZ level. [c] For linear reactants and linear products (see text). [d] Derived using eq 4 with $D_0(H-C_{2n}^-)$ from D_2O threshold measurements and experimental electron affinities from Table 1. [e] CCSD(T)/aug-cc-pVQZ//B3LYP/aug-cc-pVTZ. [f] Calculation using eq 4 with theoretical $D_0(H-C_{2n}^-)$ values and experimental electron affinities from Table 1 (see text). [g] Values adopted for combustion kinetics modeling by Kiefer et al.[1]

anion followed by a barrier to the $HCC^-\cdots HO$ complex and on to products. For NH_3, the system first passes through a shallow intermediate $C_2H^-\cdots NH_2$ ion−molecule complex, and then goes down to the $^-C{=}CHNH_2$ molecular anion followed by a second ion−molecule complex and products. For CH_4, the exit channel for the hydrogen atom transfer reaction passes through a $C_2H^-\cdots CH_3$ ion−molecule complex, with apparently only an indirect connection with the $^-C{=}CHCH_3$ molecular anion (i.e., no direct path was found in limited searches). Because the initial hydrogen atom transfer barrier is likely to be the bottleneck on the potential energy surfaces for the reactions studied here, these variations of the surfaces in the exit channel are expected to have at most a minor influence on the dynamics. Once the hydrogen atom transfer barrier region has been crossed, the systems can follow high-energy dissociative trajectories without necessarily passing through each of the intermediates shown in the exit channels.

We would expect that the potential energy surfaces for hydrogen atom transfer reactions with C_4^- and C_6^- would have qualitatively similar features as C_2^- in the entrance channel, although they might well exhibit additional intermediate structures beyond the transition state.

5. Ab Initio Energy Calculations

We have also performed higher-level ab initio calculations of the energies of linear HC_{2n}, HC_{2n}^-, C_{2n}, and C_{2n}^- ($n = 1$, 2, 3) species. These calculations are at the CCSD(T)/aug-cc-pVQZ//CCSD(T)/aug-cc-pVTZ level, i.e., using coupled cluster theory with single and double excitations and non-iterative inclusion of triples[72] and the augmented correlation-consistent basis sets of Dunning and co-workers.[67,68] Single-point energies with the quadruple-ζ basis set (QZ) were calculated at the geometries optimized with the triple-ζ basis set (TZ) constrained to linear $D_{\infty h}$ or $C_{\infty v}$ geometries. Vibrational zero-point energies are included using unscaled frequencies from B3LYP/aug-cc-pVTZ calculations. The geometries, total energies, and frequencies are included in the Supporting Information. The theoretical results for $D_0(H-C_{2n})$, $D_0(H-C_{2n}^-)$, $EA(C_{2n})$, and $EA(HC_{2n})$ are compared with experiments in Tables 1 and 3. We were unable to complete the geometry optimization at the CCSD(T) level for neutral HC_6 with available computational facilities because of its large size and low symmetry, however, so for its electron affinity and dissociation energy we have substituted CCSD(T)/aug-cc-pVQZ//B3LYP/aug-cc-pVTZ values.

The calculated electron affinities for C_{2n} ($n = 1$, 2, 3) and HC_2 are within 5 kJ/mol of the experimental values. However, the electron affinities for HC_4 and HC_6 deviate from experiment by 9 kJ/mol and 16 kJ/mol, respectively, which may be attributed to the difficulty of describing the electronic structure of these radicals as well as the lower level of calculation for HC_6. The CCSD(T) calculations for the HC_4 and HC_6 radicals exhibit serious spin contamination ($\langle S^2 \rangle$ values are included in the Supporting Information), which calls these calculations into question.[73,74] The other open-shell species also exhibit some spin contamination, but to a much smaller degree. To avoid these issues with the calculations for the neutral HC_{2n} radicals, we also determine their bond dissociation energies using the calculated values for the anions, $D_0(H-C_{2n}^-)$, and use experimental electron affinities in eq 4 to obtain estimates for $D_0(H-C_{2n})$. These alternative combined theoretical and experimental values are presented in Table 3.

6. Thermochemistry

The experimental lower limits to the bond dissociation energies for HC_{2n}^- and values for HC_{2n} derived using eq 4 are summarized and compared with theory in Table 3. Because the electron affinities used in eq 4 are taken from photoelectron spectra, which relate to vertical detachment transitions from the linear anionic molecules, our reported lower-limit values for the neutral C−H bond dissociation energies refer to *linear* HC_{2n} with *linear* C_{2n} products for $n = 2$ and $n = 3$. The neutral HC_{2n} radicals are known to have linear ground states.[15,18,52] Recent theoretical work suggests that neutral C_4 and C_6 may actually have cyclic ground-state structures, however, even though most experiments have identified the linear or pseudolinear isomers (which are favored entropically at higher temperatures and under some kinetic conditions).[34,36,51,75−78] Taking into account the energy difference of 54 ± 8 kJ/mol between the cyclic and linear form of C_6 from coupled-cluster calculations by Martin and Taylor,[77] we can estimate $D_0(H-C_6) \geq 351 \pm 14$ kJ/mol for the process forming the cyclic product isomer. However, the dissociation energies in Table 3 refer exclusively to the linear reactants and linear products.

From the threshold energy for $C_2^- + D_2O$, our experimental value for the C−H bond dissociation energy of the neutral ethynyl radical is $D_0(H-C_2) \geq 460 \pm 15$ kJ/mol (Table 3). This may be compared with a value derived from eq 6 for $n = 1$.

$$D_0(H-C_{2n}) = \Delta_f H_0(C_{2n}) - D_0(HC_{2n}-H) - \Delta_f H_0(HC_{2n}H) + 2\Delta_f H_0(H) \quad (6)$$

Using the bond dissociation energy of acetylene from photofragment translational spectroscopy,[79] $D_0(HCC-H) = 551.2 \pm 0.1$ kJ/mol, and enthalpies of formation from Table 1, eq 6 yields $D_0(H-C_2) = 470 \pm 8$ kJ/mol. An independent limit for $D_0(H-C_2)$ has been reported from two-photon laser-induced fluorescence of HCCH by Jackson and co-workers,[13] $D_0(H-C_2) < 112 \pm 0.7$ kcal/mol = 468.6 ± 3.3 kJ/mol as reported or revised to $D_0(H-C_2) < 467 \pm 3$ kJ/mol using the value of $D_0(HCC-H)$ given above. The value we obtain from coupled cluster theory is $D_0(H-C_2) = 464.5$ kJ/mol, or $D_0(H-C_2) = 471$ obtained by combining the theoretical $D_0(H-C_2^-)$ with experimental electron affinities (Table 3). The present experimental lower limit of $D_0(H-C_2) \geq 460 \pm 15$ kJ/mol is consistent with these values and implies that any excess reaction threshold energy above the reaction endothermicity is small, $<(10 \pm 15)$ kJ/mol, for the $C_2^- + D_2O$ deuterium atom transfer reaction.

The reasonable limit obtained for $D_0(H-C_2)$ offers some hope that the present lower limits for $D_0(H-C_4)$ and $D_0(H-C_6)$ obtained from the reactions of C_4^- and C_6^- with D_2O, respectively, are also close to the true thermochemical values. For HC_4 and HC_6, precise comparisons using eq 6 cannot be obtained because enthalpies of formation of the parent polyynes are not known experimentally. However, Dorofeeva and Gurvich[33] have estimated the enthalpies of formation of HC_4H and HC_6H using group additivity (values given in Table 1). Experimental gas-phase acidities[80,81] for HC_4H and HC_6H can be combined with known electron affinities of $C_{2n}H$ (Table 1) to provide dissociation energies of $D_0(HC_4-H) = 539 \pm 12$ kJ/mol and $D_0(HC_6-H) = 535 \pm 13$ kJ/mol. Using eq 6 with these values yields estimates of $D_0(H-C_4) = 496 \pm 28$ kJ/mol and $D_0(H-C_6) = 543 \pm 45$ kJ/mol, which are 68 and 133 kJ/mol larger than our experimental lower limits. Unfortunately, the theoretical calculations are not too helpful in resolving the true values, as they give $D_0(H-C_4) = 470$ kJ/mol and $D_0(H-C_6) = 474$ kJ/mol (using calculated anion dissociation energies and experimental electron affinities), i.e., in agreement within the experimental uncertainties for $D_0(H-C_4)$ but not for $D_0(H-C_6)$. These deviations could arise from either experimental or theoretical sources. First, the assumptions of group additivity might well not apply for the longer polyynes. For the present experiments (which as *lower limits* agree with the other experiments and theory), it is possible that the potential energy surfaces for hydrogen atom transfer reaction exhibit a higher-energy or more restrictive transition state for the longer-chain carbon cluster anions than for C_2^-. Regarding the accuracy of the ab initio energies, we have noted above the difficulties of properly describing the neutral C_{2n} and $C_{2n}H$ species because of spin contamination and mixing of cumulenic and acetylenic electronic configurations. Nevertheless, our new experimental values for $D_0(H-C_4)$ and $D_0(H-C_6)$ provide firm lower limits that are significant *higher* than values adopted for kinetic modeling of acetylene pyrolysis by Kern et al.,[1] which are listed in Table 3 for comparison. It is clear that further experimental and theoretical work on the energetics of these radicals is needed to pin down their thermochemistry. In the meantime, it is our judgment that the combined theoretical and experimental estimates for $D_0(H-C_4)$ and $D_0(H-C_6)$ in Table 3 represent the best currently available values, but it is difficult to assign error limits. We reiterate that these dissociation energies all refer to linear reactant and linear product geometries.

7. Conclusion

The thermochemical results of the present work are summarized in Table 3. The reported C−H dissociation energies for HC_{2n} and HC_{2n}^- refer to linear reactant and linear product species. The measured values or reaction threshold energies are strictly upper limits for the enthalpies of reaction and therefore the derived experimental values of $D(H-C_{2n}^-)$ and $D(H-C_{2n})$ are lower limits. For $n = 1$, $D_0(H-C_2)$ is in good agreement with theory and independent measurements, which indicates that there is at most a small excess threshold energy in that case. However, for $D_0(H-C_4)$ and $D_0(H-C_6)$, the values are significantly smaller than theory and other available experimental estimates, i.e., in agreement as lower limits but implying that the hydrogen atom transfer reactions of C_4^- and C_6^- with D_2O do exhibit excess energy thresholds (i.e., reverse activation energies for translation excitation). Nevertheless, the experimental values even as lower limits represent a significant improvement over estimates previously used for modeling acetylene combustion kinetics.[1] This work further underscores the need to use multiple reagents to validate threshold energy measurements for thermochemical determinations, or else to uncover reverse activation energies as found here.

The energy barriers for hydrogen atom transfer found in the present calcuations (Figure 4) explain why C_{2n}^- species are unreactive with many small hydrogen containing molecules under thermal conditions,[39−41] as discussed in the Introduction. The nonreactivity of anionic carbon chain with molecular hydrogen has important consequences for the abundances of C_n^- and C_nH^- in insterstellar environments.[41] If $D_0(C_{2n}-H^-)$ is larger than or equal to $D_0(H_2) = 432$ kJ/mol,[82] as the experiments for $n = 1$ and the calculations for $n = 2$ and $n = 3$ suggest, then the nonreactivity[41] of C_{2n}^- with H_2 is due to an energy barrier for the hydrogen atom transfer process. Fundamentally, the barrier for hydrogen atom transfer in these systems results from an avoided crossing of electronic states corresponding to the $\cdot C_{2n}^- + HX$ and $C_{2n}H^- + X\cdot$ configurations, where HX and $C_{2n}H^-$ are closed-shell singlets. In contrast, gas-phase proton-transfer reactions of anions usually exhibit a deep well corresponding to the $[A^-\cdot-H^+-B^-]$ intermediate, due to the ease with which the proton shares electrons in forming hydrogen bonds with both electron donors.

Acknowledgment. This research is supported by the Department of Energy, Basic Energy Sciences, Chemical Sciences, Geosciences and Biosciences Division.

Supporting Information Available: Calculated geometries and molecular parameters used for fits and thermal corrections. This material is available free of charge via the Internet at http://pubs.acs.org.

References and Notes

(1) Kiefer, J. H.; Sidhu, S. S.; Kern, R. D.; Xie, K.; Chen, H.; Harding, L. B. *Combust. Sci. Tech.* **1992**, *82*, 101.
(2) Zhang, H.-Y.; McKinnon, J. T. *Combust. Sci. Tech.* **1995**, *107*, 261.
(3) Kruse, T.; Roth, P. *J. Phys. Chem. A* **1997**, *101*, 2138.
(4) Guélin, M.; Green, S.; Thaddeus, P. *Astrophys. J.* **1978**, *224*, L27.
(5) Pauzat, F.; Ellinger, Y.; McLean, A. D. *Astrophys. J.* **1991**, *369*, L13.
(6) Fulara, J.; Lessen, D.; Freivogel, P.; Maier, J. P. *Nature* **1993**, *366*, 439.
(7) Cernicharo, J.; Guélin, M. *Astron. Astrophys.* **1996**, *309*, L27.
(8) Ervin, K. M.; Lineberger, W. C. *J. Phys. Chem.* **1991**, *95*, 1167.
(9) Taylor, T. R.; Xu, C.; Neumark, D. M. *J. Chem. Phys.* **1998**, *108*, 10018.
(10) Pino, T.; Tulej, M.; Güthe, F.; Pachkov, M.; Maier, J. P. *J. Chem. Phys.* **2002**, *116*, 6126.
(11) Shepherd, R. A.; Graham, W. R. M. *J. Chem. Phys.* **1987**, *86*, 2600.
(12) Brown, J. M.; Evenson, K. M. *J. Mol. Spectrosc.* **1988**, *131*, 161.
(13) Urdahl, R. S.; Bao, Y.; Jackson, W. M. *Chem. Phys. Lett.* **1991**, *178*, 425.
(14) Hsu, Y.-C.; Lin, J. J.-M.; Papousek, D.; Tsai, J.-j. *J. Chem. Phys.* **1993**, *98*, 6690.
(15) Linnartz, H.; Motylewsi, T.; Vaizert, O.; Maier, J. P.; Apponi, A. J.; McCarthy, M. C.; Gottlieb, C. A.; Thaddeus, P. *J. Mol. Spectrosc.* **1999**, *197*, 1.
(16) Woon, D. E. *Chem. Phys. Lett.* **1995**, *244*, 45.
(17) Sobolewski, A. L.; Adamowicz, L. *J. Chem. Phys.* **1995**, *102*, 394.
(18) Natterer, J.; Koch, W. *Mol. Phys.* **1995**, *84*, 691.
(19) McCarthy, M. C.; Gottlieb, C. A.; Thaddeus, P.; Horn, M.; Botschina, P. *J. Chem. Phys.* **1995**, *103*, 7820.
(20) Brown, S. T.; Rienstra-Kiracofe, J. C.; Schaefer, H. F., III. *J. Phys. Chem. A* **1999**, *103*, 4065.
(21) Graf, S.; Geiss, J.; Leutwyler, S. *J. Chem. Phys.* **2001**, *114*, 4542.
(22) Szalay, P. G.; Tajti, A.; Stanton, J. F. *Mol. Physics* **2005**, *103*, 2159.
(23) McCarthy, M. C.; Gottlieb, C. A.; Gupta, H.; Thaddeus, P. *Astrophys. J.* **2006**, *652*, L141.
(24) Cernicharo, J.; Guelin, M.; Agundez, M.; Kawaguchi, K.; McCarthy, M.; Thaddeus, P. *Astron. Astrophys.* **2007**, *467*, L37.
(25) Brünken, S.; Gupta, H.; Gottlieb, C. A.; McCarthy, M. C.; Thaddeus, P. *Astrophys. J.* **2007**, *664*, L43.

(26) Gupta, H.; Brünken, S.; Tamassia, F.; Gottlieb, C. A.; McCarthy, M. C.; Thaddeus, P. *Astrophys. J.* **2007**, *655*, L57.
(27) Arnold, D. W.; Bradforth, S. E.; Kitsopoulos, T. N.; Neumark, D. M. *J. Chem. Phys.* **1991**, *95*, 8753.
(28) Arnold, C. C.; Zhao, Y.; Kitsopoulos, T. N.; Neumark, D. M. *J. Chem. Phys.* **1992**, *97*, 6121.
(29) DeTuri, V. F.; Hintz, P. A.; Ervin, K. M. *J. Phys. Chem. A* **1997**, *101*, 5969.
(30) Ervin, K. M. *Chem. Rev.* **2001**, *101*, 391. Erratum, Ervin, K. M. *Chem. Rev.* **2002**, *102*, 855.
(31) Ervin, K. M.; Gronert, S.; Barlow, S. E.; Gilles, M. K.; Harrison, A. G.; Bierbaum, V. M.; DePuy, C. H.; Lineberger, W. C.; Ellison, G. B. *J. Am. Chem. Soc.* **1990**, *112*, 5750.
(32) Gurvich, L. V.; Veyts, I. V.; Alcock, C. B. *Thermodynamic Properties of Individual Substances*, 4th ed., Vol. 2 (Elements C, Si, Ge, Sn, Pb, and Their Compounds), Parts 1−2; Hemisphere: New York, 1991.
(33) Dorofeeva, O. A.; Gurvich, L. V. *Thermochem. Acta* **1991**, *178*, 273.
(34) Gingerich, K. A.; Finkbeiner, H., C.; Schmude, R. W., Jr. *Chem. Phys. Lett.* **1993**, *207*, 23.
(35) Berkowitz, J.; Ellison, G. B.; Gutman, D. *J. Phys. Chem.* **1994**, *98*, 2744.
(36) Gingerich, K. A.; Finkbeiner, H. C.; Schmude, R. W., Jr. *J. Am. Chem. Soc.* **1994**, *116*, 3884.
(37) Ruscic, B.; Boggs, J. E.; Burcat, A.; Csaszar, A. G.; demaison, J.; Janoschek, R.; Martin, J. M. L.; Morton, M. L.; Rossi, M. J.; Stanton, J. F.; Szalay, P. G.; Westmoreland, P. R.; Zabel, F.; Berces, T. *J. Phys. Chem. Ref. Data* **2005**, *34*, 573.
(38) Bodi, A.; Kercher, J. P.; Bond, C.; Meteesatien, P.; Sztaray, B.; Baer, T. *J. Phys. Chem. A* **2006**, *110*, 13425.
(39) Schiff, H. I.; Bohme, D. K. *Int. J. Mass Spectrom. Ion Phys.* **1975**, *1975*, 167.
(40) Payzant, J. D.; Tanaka, K.; Betowski, L. D.; Bohme, D. K. *J. Am. Chem. Soc.* **1976**, *98*, 894.
(41) Barckholtz, C.; Snow, T. P.; Bierbaum, V. M. *Astrophys. J.* **2001**, *547*, L171.
(42) Hopwood, F. G.; Fisher, K. J.; Willet, G. D.; Greenhill, P. G. *Rapid Commun. Mass Spectrom.* **1996**, *10*, 110.
(43) Fisher, K.; Hopwood, F.; Dance, I.; Willet, G. *New J. Chem.* **1999**, *23*, 609.
(44) Armentrout, P. B. *Int. Rev. Phys. Chem.* **1990**, *9*, 115.
(45) Armentrout, P. B. Thermochemical Measurements by Guided Ion Beam Mass Spectrometry. In *Advances in Gas Phase Ion Chemistry*; Adams, N. G., Babcock, L. M., Eds.; JAI Press: Greenwich, CT, 1992; Vol. 1, p 83.
(46) Angel, L.; Ervin, K. *J. Phys. Chem. A* **2001**, *105*, 4042.
(47) Mann, D. J.; Hase, W. L. *J. Phys. Chem. A* **1998**, *102*, 6208.
(48) Yang, S.; Taylor, K. J.; Craycraft, M. J.; Conceicao, J.; Pettiette, C. L.; Cheshnovsky, O.; Smalley, R. E. *Chem. Phys. Lett.* **1988**, *144*, 431.
(49) Xu, C.; Burton, G. R.; Taylor, T. R.; Neumark, D. M. *J. Chem. Phys.* **1997**, *107*, 3428.
(50) von Helden, G.; Kemper, P. R.; Gotts, N. G.; Bowers, M. T. *Science* **1993**, *259*, 1300.
(51) Raghavachari, K. *Z. Phys. D - At. Molec. Clusters* **1989**, *12*, 61.
(52) Pan, L.; Rao, B. K.; Gupta, A. K.; Das, G. P.; Ayyub, P. *J. Chem. Phys.* **2003**, *119*, 7705.
(53) Watts, J. D.; Cernusak, I.; Bartlett, R. J. *Chem. Phys. Lett.* **1991**, *178*, 259.
(54) Watts, J. D.; Gauss, J.; Stanton, J. F.; Bartlett, R. J. *J. Chem. Phys.* **1992**, *97*, 8372.
(55) Szczepanski, J.; Kern, S. E.; Vala, M. *J. Phys. Chem. A* **1997**, *101*, 1841.
(56) Adamowicz, L. *Chem. Phys.* **1991**, *156*, 387.
(57) Adamowicz, L. *Chem. Phys. Lett.* **1991**, *182*, 45.
(58) Ervin, K. M.; Armentrout, P. B. *J. Chem. Phys.* **1985**, *83*, 166.
(59) Rodgers, M. T.; Ervin, K. M.; Armentrout, P. B. *J. Chem. Phys.* **1997**, *106*, 4499.
(60) Armentrout, P. B.; Ervin, K. M. CRUNCH, Fortran program, (University of Utah, Salt Lake City, and University of Nevada, Reno), version 5.1 (2007).
(61) Lifshitz, C.; Wu, R.; Tiernan, T. O.; Terwilleger, D. T. *J. Chem. Phys.* **1978**, *68*, 247.
(62) Dalleska, N. F.; Honma, K.; Sunderlin, L. S.; Armentrout, P. B. *J. Am. Chem. Soc.* **1994**, *116*, 3519.
(63) DeTuri, V. F.; Su, M. A.; Ervin, K. M. *J. Phys. Chem. A* **1999**, *103*, 1468.
(64) Grushow, A.; Ervin, K. M. *J. Chem. Phys.* **1997**, *106*, 9580. Grushow, A.; Ervin, K. M. *J. Chem. Phys.* **1997**, *107*, 8210.
(65) Taylor, B. N.; Kuyatt, C. Guidelines for Evaluating and Expressing the Uncertainty of NIST Measurement Results, NIST Technical Note 1297, Washington, DC: National Institute of Standards and Technology, 1994. (http://physics.nist.gov/Document/tn1297.pdf, accessed 12/1/2004).
(66) Lee, C.; Yang, W.; Parr, R. G. *Phys. Rev. B* **1988**, *37*, 785.
(67) Dunning, T. H., Jr. *J. Chem. Phys.* **1989**, *90*, 1007.
(68) Kendall, R. A.; Dunning, T. H., Jr.; Harrison, R. J. *J. Chem. Phys.* **1992**, *96*, 6792.
(69) Frisch, M. J.; Trucks, G. W.; Schlegel, H. B.; Scuseria, G. E.; Robb, M. A.; Cheeseman, J. R.; Montgomery, J. A., Jr.; Vreven, T.; Kudin, K. N.; Burant, J. C.; Millam, J. M.; Iyengar, S. S.; Tomasi, J.; Barone, V.; Mennucci, B.; Cossi, M.; Scalmani, G.; Rega, N.; Petersson, G. A.; Nakatsuji, H.; Hada, M.; Ehara, M.; Toyota, K.; Fukuda, R.; Hasegawa, J.; Ishida, M.; Nakajima, T.; Honda, Y.; Kitao, O.; Nakai, H.; Klene, M.; Li, X.; Knox, J. E.; Hratchian, H. P.; Cross, J. B.; Bakken, V.; Adamo, C.; Jaramillo, J.; Gomperts, R.; Stratmann, R. E.; Yazyev, O.; Austin, A. J.; Cammi, R.; Pomelli, C.; Ochterski, J. W.; Ayala, P. Y.; Morokuma, K.; Voth, G. A.; Salvador, P.; Dannenberg, J. J.; Zakrzewski, V. G.; Dapprich, S.; Daniels, A. D.; Strain, M. C.; Farkas, O.; Malick, D. K.; Rabuck, A. D.; Raghavachari, K.; Foresman, J. B.; Ortiz, J. V.; Cui, Q.; Baboul, A. G.; Clifford, S.; Cioslowski, J.; Stefanov, B. B.; Liu, G.; Liashenko, A.; Piskorz, P.; Komaromi, I.; Martin, R. L.; Fox, D. J.; Keith, T.; Al-Laham, M. A.; Peng, C. Y.; Nanayakkara, A.; Challacombe, M.; Gill, P. M. W.; Johnson, B.; Chen, W.; Wong, M. W.; Gonzalez, C.; Pople, J. A. *Gaussian 03*, revision C.02, Wallingford, CT: Gaussian, Inc. 2004.
(70) Baboul, A. G.; Schelgel, H. B. *J. Chem. Phys.* **1997**, *107*, 9413.
(71) Angel, L. A.; Ervin, K. M. *J. Am. Chem. Soc.* **2003**, *125*, 1014.
(72) Pople, J. A.; Head-Gordon, M.; Raghavachari, K. *J. Chem. Phys.* **1987**, *87*, 5968.
(73) Stanton, J. F. *J. Chem. Phys.* **1994**, *101*, 371.
(74) Beran, G. J. O.; Gwaltney, S. R.; Head-Gordon, M. *Phys. Chem. Chem. Phys.* **2003**, *5*, 2488.
(75) Hwang, H. J.; Van Orden, A.; Tanaka, K.; Kuo, E. W.; Heath, J. R.; Saykally, R. J. *Mol. Phys.* **1993**, *79*, 769.
(76) Van Orden, A.; Saykally, R. J. *Chem. Rev.* **1998**, *98*, 2313.
(77) Martin, J. M. L.; Taylor, P. R. *J. Phys. Chem.* **1996**, *100*, 6047.
(78) Jones, R. O. *J. Chem. Phys.* **1999**, *110*, 5189.
(79) Mordaunt, D. H.; Ashfold, M. N. R. *J. Chem. Phys.* **1994**, *101*, 2630.
(80) Shi, Y.; Ervin, K. M. *Chem. Phys. Lett.* **2000**, *318*, 149.
(81) Natterer, J.; Koch, W.; Schröder, D.; Goldberg, N.; Schwarz, H. *Chem. Phys. Lett.* **1994**, *229*, 429.
(82) Gurvich, L. V.; Veyts, I. V.; Alcock, C. B. *Thermodynamic Properties of Individual Substances*, 4th ed., Vol. 1 (Elements O, H (D, T), F, Cl, Br, I, He, Ne, Ar, Kr, Xe, Rn, S, N, P and Their Compounds), Parts 1−2; Hemisphere Publishing Corporation: New York, 1989.